RSC Advances

ROYAL SOCIETY OF CHEMISTRY

www.rsc.org/advances

Preparation and electromagnetic wave absorption properties of novel dendrite-like NiCu alloy composite

Biao Zhao [a], Gang Shao [a] *, Bingbing Fan [a], Wanyu Zhao [a], Rui Zhang [a, b] *

Received (in XXX, XXX) Xth XXXXXXXXX 20XX, Accepted Xth XXXXXXXXX 20XX
DOI: 10.1039/c000000x

A novel leaf-like NiCu alloy composite was prepared by a simple solution reduction method. The dendritic hierarchical structures were composed of main stem with several micrometers and plentiful branches. The NiCu paraffin-composite containing 40 wt% NiCu dendrite exhibits excellent microwave absorption properties. The minimal reflection loss(RL) of -21.1 dB can be observed at 14.9 GHz and the bandwidth with RL less than -10 dB reaches 3.4 GHz (13.4-16.8 GHz) with only thickness of 1.4 mm. This novel dendrite-like NiCu alloy could be used as a promising absorbing material with low thickness, high absorption and wide-band as well as easy preparation.

Over the past years, electromagnetic pollution has become a serious problem due to the fast development of electronic products and communication devices. As a consequence, suitable electromagnetic wave absorption materials which have strong microwave absorption over a broad frequency spectrum are attracted a great deal of attention.[1-3] It is well known that the shapes of materials play an important role on microwave absorption capabilities. [4, 5] Recently, the materials with dendrite-like hierarchical structures have shown outstanding microwave absorption properties.[6-9] For example, the dendritic α-Fe was synthesized by an electric field-induced and the α-Fe exhibits high absorption efficiency with the minimum reflection loss value of –32.3 dB. [7] Yu et al. prepared leaf-like Co_xFe_{1-x} (x =0.1, 0.3, 0.5 and 0.7) alloys and the leaf-like dendritic $Co_{0.5}Fe_{0.5}$ alloy exhibits the strongest microwave absorption with minimal reflection loss of −59.1 dB. [6] In these dendrite-like hierarchical structures, the high surface areas of dendrites can tune the electromagnetic parameters to obtain good impedance match. On the other hand, the unique leaf-like structures can induce formation of vibrating microcurrent, which is beneficial for microwave absorption. [10]

However, to best of our knowledge, the reports on the preparation and microwave absorption of NiCu microspheres are rare.[11] In this manuscript, a novel dendrite-like NiCu alloy, which has low cost, strong absorption, thin thickness and a wide absorption band in the microwave frequency, has been prepared through a facile hydrothermal method. This novel leaf-like NiCu alloy can be used as a promising absorbing material.

Leaf-like NiCu alloy composite was synthesized by a facile liquid phase process. Firstly, 0.001mol $CuCl_2{\cdot}2H_2O$ and 0.001mol $NiCl{\cdot}6H_2O$ were dissolved in 60 mL H_2O and magnetic stirring vigorously for 15 min. Then, 4.8 g NaOH was introduced into the above mixture. Afterwards, 5 mL ethanediamine and 0.01 mol sodium hypophosphite monohydrate ($NaH_2PO_2{\cdot}H_2O$) were added into the solution respectively whilst stirring for 30min, the above solution was transferred into a Teflon-lined stainless-steel autoclave and kept at 140 °C for 15 h. After cooled to room temperature, the final products were washed with distilled water and absolute ethanol for several times and dried for 8 h in vacuum. The formation of the NiCu alloy depends on the following redox reactions:

$$2Cu^{2+} + H_2PO_2^- + 4OH^- \rightarrow Cu + PO_3^- + 3H_2O \quad (1)$$

$$2Ni^{2+} + H_2PO_2^- + 4OH^- \rightarrow Ni + PO_3^- + 3H_2O \quad (2)$$

The crystal phase of the obtained powder was determined by powder X-ray diffraction (XRD) analysis. The XRD pattern of the dendrite-like NiCu alloys sample is shown in Figure 1. From the Figure 1, the three peaks at 2θ = 43.52, 50.84 and 74.98 are in an intermediate position in relation to the peaks corresponding to the pure Cu (JCPDS file nos. 04-0836) and Ni metals (JCPDS file nos. 04-0836). which can validate the single face centered cubic (fcc) structure of the bimetallic nanoalloy. These results suggest that a Cu–Ni alloy was formed by means of the substitution of Cu by Ni. Cu–Ni alloys are basically a solid solution formed by the substitution of Cu by Ni because both metals have the same, crystalline structure, ionic radius

electronegativity and identical valence, which will be favor of meeting the Hume–Rothery rules for a substitutional solid solution.[11, 12]

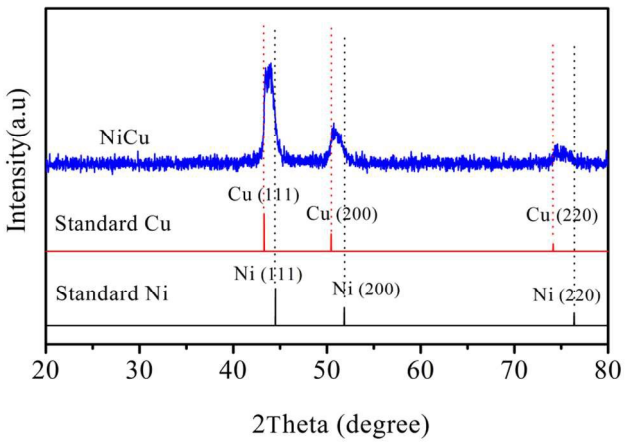

Fig. 1 XRD pattern of NiCu products obtained at 140 °C for 15 h.

Typical FESEM images of the as-obtained NiCu alloy composite with different magnifications are presented in Figure 2(a,b). Figure 2a is the low magnification FESEM photograph of the sample, which indicates the obtained product is composed of novel dendritic superstructures with an average diameter of ca. 10 μm. A magnified image of an individual NiCu alloy was shown in Figure 2b. It can be clearly observed that on the dendritic hierarchical structures, several leaves (first branches) with different lengths and widths are connected to the main branch. The length of the main branch is several micrometers, and that of each leaf (second branches) is about 1–2 μm with a width ranging from 300 to 600 nm. Interestingly, close inspection of the dendritic hierarchical structures shows that each leaf connected to the main branch also acts as a secondary main branch to be connected by smaller leaves (tertiary branches). X-ray energy dispersive spectroscopy (EDS) microanalysis of the dendrite-like NiCu alloy displays that the as-received sample is essentially comprised of Ni and Cu (Figure 2c). Only a very small amount of oxygen is detected, which may be due to slight oxidation of the surface. The molar ratio of Ni to Cu is about 1.1:1, which is nearly 1:1. Figure 2d exhibits the transmission electron microscopy (TEM) images of the as-synthesized NiCu sample. The NiCu alloys with dendrites can be clearly seen in Figure 2d.

To get more information about Ni-Cu alloy, the mapping data of Cu and Ni elements were shown in Figure S1. Both of Cu atoms and Ni atoms show an uniform distribution in accordance with the shape of the examined fractal, which indicates that the alloy is a homogenous phase.

In this work, the ethanediamine plays a vital role in determining the morphology of final NiCu alloy. For comparison, the NiCu alloy composites without ethanediamine were synthesized and the results were shown in Figure S2. It can be clearly observed that the NiCu alloys prepared without ethanediamine are comprised of plentiful aggregated nanoparticles. In present synthesis, a strong basic condition was adopted, and the two metallic complexes ($Ni(OH)_4^{2-}$, $Cu(OH)_4^{2-}$) were formed. When the ethanediamine was introduced into this reaction, complexes such as $Cu(OH)_4^{2-}$ and $Cu(EDA)_2^{2+}$ are supposed to be present in solution precursors, together with $Ni(EDA)_3^{2+}$. These complexes are expected to control the redox rate by slow release of metal ions , which cause formation special dendrite-like structures.

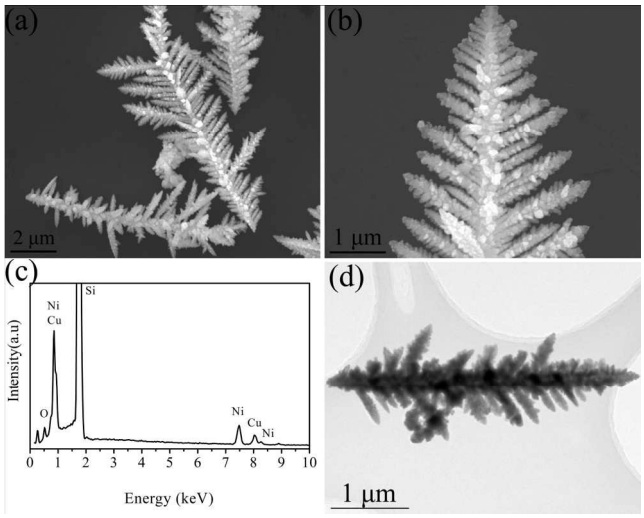

Fig. 2 (a,b) Different magnification FESEM images, (c) EDS profile and (d) TEM images of dendrite-like NiCu alloy composite

Figure S3 shows the magnetic hysteresis loops (M–H loops) combined with the expanded low-field hysteresis curves (inset of Fig. S3) of NiCu alloy measured at room-temperature, which indicate the magnetic properties, including saturation

magnetization Ms and coercivities Hc, respectively. As can be seen, the three samples exhibit typical soft ferromagnetism. The Ms value of NiCu is about 27.5 emu/g, which is lower than the value of Ni (58.57 emu/g). The decrease in the magnetization is mainly attributed to the existence of nonmagnetic Cu component in alloy.

The microwave absorption properties were mainly associated with the complex relative permittivity ($\varepsilon_r = \varepsilon' - j\varepsilon''$) and permeability ($\mu_r = \mu' - j\mu''$) as well as their mass ration in the paraffin-composite. [13, 14] Figure 3 presents the frequency-dependent electromagnetic parameters of the paraffin-composite with various NiCu alloy loadings. The real parts of the complex permittivity and permeability represent the storage of electric and magnetic energies, whereas the imaginary parts symbolize the loss of both energies.[15] From the Figure 3a, the real parts (ε′) of NiCu paraffin-composites increase with increasing the NiCu alloy loadings. This result can be explained by the high electrical conductivity of NiCu at high loading that enables strong polarization due to the presence of dipoles and other bound charges, leading to improved ε′. Notably, the imaginary part (ε″) of complex permittivity shows the similar trend with the real part (ε′). The ε″ values of NiCu paraffin-composites show the increase tendency with increasing NiCu alloy contents (Figure 3b). According to the free-electron theory [16, 17], $\varepsilon'' \approx 1/\pi\varepsilon_0\rho f$, where ρ is the resistivity, the high ε″ indicates the high conductivity. The high ε″ value of NiCu paraffin-composite with 50 wt% NiCu implies the high conductivity, which maybe suggests high dielectric loss of microwave. It is well known that one of the key conditions to achieve a low reflection is the impedance matching that the microwave can enter into the absorber as much as possible. However, too high values of complex permittivity could lead to bad impedance match between absorber and air, which will result in more microwave reflection rather than absorption. Thus, the materials with the appropriate conductivity favor microwave absorption. [18, 19]

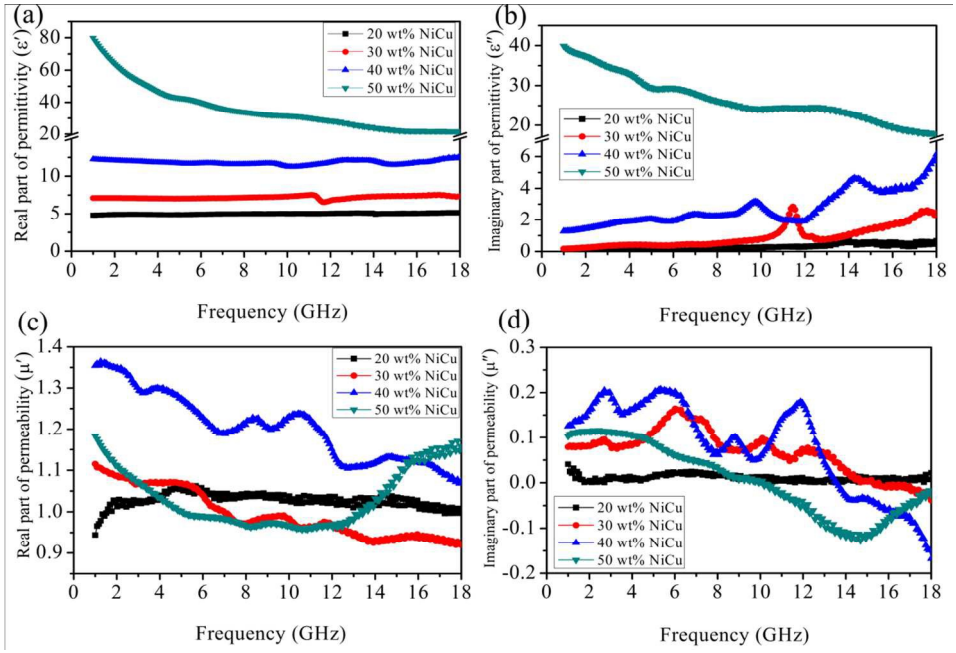

Fig. 3 Frequency dependence of (a) real parts and (b) imaginary parts of complex permittivity, and (c) real parts and (d) imaginary parts of complex permeability of various NiCu paraffin-composite.

Figure 3(c,d) shows the complex permeability, real part μ′, and imaginary part μ″ of NiCu paraffin-composite with various NiCu loadings in the frequency of 1–18 GHz. The paraffin-composite with 40 wt% NiCu contents shows the high μ′ values compared with other three paraffin-composite. In Figure 3d, the μ″ values of four paraffin-composite exhibit decline trend with increasing the

measured frequency. Notably, the 30wt% NiCu and 30wt% NiCu paraffin composites show multiple peaks in the μ″ curves, which are attributed to natural and exchange resonances.[20, 21] Moreover, it is interesting to note that the paraffin-composites with high CuNi loadings (30 wt%, 40 wt%, 50 wt%) signify negative μ″ values in the high frequency (12-18 GHz). This can be explained that magnetic energy is radiated out and transferred into the electric energy. [22, 23]

Reflection loss (RL) of the NiCu paraffin-composite can be calculated based on Eqn (3) and Eqn (4). The microwave absorbance of the samples can be predicted from the value of RL in which the larger the negative value of RL, the greater the microwave absorption properties of materials. [13, 24]

$$RL = 20\log_{10}\left|(Z_{in} - Z_0)/(Z_{in} + Z_0)\right| \quad (3)$$

$$Z_{in} = Z_0\sqrt{\frac{\mu_r}{\varepsilon_r}}\tanh\left(j\frac{2\pi fd\sqrt{\mu_r\varepsilon_r}}{c}\right) \quad (4)$$

where Z_0, Z_{in}, f, c, and d are the impedance of free space, input impedance of the absorber, the measured frequency, the velocity of electromagnetic waves, the absorber thickness. Figure 4a depicts the reflection losses of various NiCu paraffin composites with absorber thickness of 1.6 mm. It can be found that the 40 wt% NiCu paraffin composite shows the best microwave absorption with the minimum RL of -20.0 dB with the thickness of 1.6 mm. The absorber thickness also affect the RL peaks and location. Thus the RL values of 40 wt% NiCu paraffin composite with different thicknesses are also calculated (Figure 4b). The optimal RL is -21.1 dB at 14.9 GHz with only thickness of 1.4 mm. The absorption bandwidth with RL below -10 dB (90% absorption) can be monitored between 6.4 GHz and 18 GHz f with the thin absorber thickness of 1.1–2.8 mm In addition, the absorption band shifts to lower frequency range if the absorber thickness increased when measuring, which is the result of quarter-wavelength cancellation. [25]

To reveal the effect of dendritic hierarchical structures on the absorption properties, the absorption behaviors of NiCu alloy without dendritic hierarchical structures which are synthesized in the absence of ethanediamine are also discussed. As shown in Figure S4, the NiCu alloy composites prepared without ethanediamine show weak microwave absorption capabilities, which exhibits the minimum reflection loss of -6.22 dB.

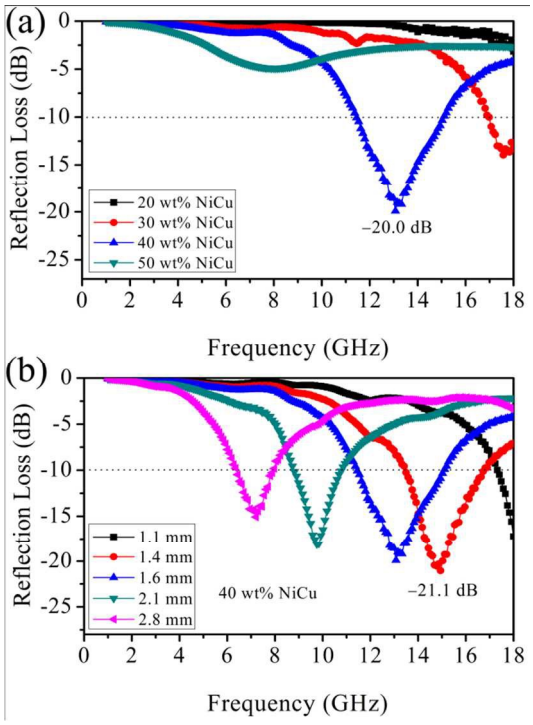

Fig. 4 (a) Reflection loss of NiCu paraffin-composites with different NiCu loadings for the thickness of 1.6 mm; (b) The simulated reflection loss of 40 wt% NiCu paraffin composite with various thicknesses.

In summary, a facile solution reduction was used to synthesize novel dendrite-like NiCu alloys. The microwave absorption properties of NiCu paraffin composites were vitally influenced by the NiCu loadings. The NiCu paraffin-composite with 40 wt% NiCu alloy exhibits outstanding microwave absorption properties. The minimum reflection loss is -21.1 dB at 14.9 GHz with only thickness of 1.4 mm. This novel leaf-like NiCu alloys may pave a way to prepare the promising absorbing materials with the features of strong absorption, small thickness and wide-band.

Acknowledgements

We acknowledge the financial supports from Natural Science Foundation of China (no. 51172213)

[a] *School of Materials Science and Engineering, Zhengzhou University, Zhengzhou 450001, China*
[b] *Laboratory of Aeronautical Composites, Zhengzhou Institute of Aeronautical Industry Management, Zhengzhou 450046, China*
** Corresponding Author.*

Dr. Gang Shao
E-mail address: gang_shao@zzu.edu.cn
Prof. Rui Zhang
Tel: +86-371-60632007
Fax: +86-371-60632600
E-mail address: zhangray@zzu.edu.cn

1. G. Tong, F. Liu, W. Wu, F. Du and J. Guan, *J. Mater. Chem. A*, 2014, **2**, 7373-7382.
2. D. Sun, Q. Zou, Y. Wang, Y. Wang, W. Jiang and F. Li, *Nanoscale*, 2014, **6**, 6557-6562.
3. W. Li, B. Lv, L. Wang, G. Li and Y. Xu, *RSC Adv.*, 2014, **4**, 55738-55744.
4. H. Li, Y. Huang, G. Sun, X. Yan, Y. Yang, J. Wang and Y. Zhang, *J. Phys. Chem. C*,, 2010, **114**, 10088-10091.
5. Q. Liu, X. Xu, W. Xia, R. Che, C. Chen, Q. Cao and J. He, *Nanoscale*, 2015, **7**, 1736-1743.
6. Z. Yu, N. Zhang, Z. Yao, X. Han and Z. Jiang, *J. Mater. Chem. A*, 2013, **1**, 12462-12470.
7. Z. Yu, Z. Yao, N. Zhang, Z. Wang, C. Li, X. Han, X. Wu and Z. Jiang, *J. Mater. Chem. A*, 2013, **1**, 4571-4576.
8. G. Sun, B. Dong, M. Cao, B. Wei and C. Hu, *Chem. Mater.*,, 2011, **23**, 1587-1593.
9. Z. Yu, Z. Yao, N. Zhang and Z. Jiang, *RSC Adv.*, 2015, **5**, 25266-25272.
10. G. Tong, J. Yuan, W. Wu, Q. Hu, H. Qian, L. Li and J. Shen, *CrystEngComm*, 2012, **14**, 2071-2079.
11. S. Kumari, A. Kumar, A. P. Singh, M. Garg, P. K. Dutta, S. K. Dhawan and R. B. Mathur, *RSC Adv.*, 2014, **4**, 23202-23209.
12. D. K. Sood, *Phys. Lett. A*, 1978, **68**, 469-472.
13. B. Zhao, G. Shao, B. Fan, W. Zhao and R. Zhang, *Phys. Chem. Chem. Phys.*, 2015, **17**, 6044-6052.
14. L. Wang, Y. Huang, C. Li, J. Chen and X. Sun, *Phys. Chem. Chem. Phys.*, 2015, **17**, 5878-5886.
15. C. Cui, Y. Du, T. Li, X. Zheng, X. Wang, X. Han and P. Xu, *J. Phys. Chem. B*, 2012, **116**, 9523-9531.
16. X. G. Liu, J. J. Jiang, D. Y. Geng, B. Q. Li, Z. Han, W. Liu and Z. D. Zhang, *Appl. Phys. Lett.*, 2009, **94**, 053119.
17. B. Zhao, G. Shao, B. Fan, W. Zhao, Y. Chen and R. Zhang, *RSC Adv.*, 2015, **5**, 9806-9814.
18. B. Zhao, G. Shao, B. Fan, W. Li, X. Pian and R. Zhang, *Mater. Lett.,* 2014, **121**, 118-121.
19. X. Li, J. Feng, H. Zhu, C. Qu, J. Bai and X. Zheng, *RSC Adv.*, 2014, **4**, 33619-33625.
20. A. Aharoni, *J. Appl. Phys.*, 1991, **69**, 7762-7764.
21. B. Zhao, G. Shao, B. Fan, W. Zhao and R. Zhang, *RSC Adv.*, 2014, **4**, 57424-57429.
22. X.-L. Shi, M.-S. Cao, J. Yuan and X.-Y. Fang, *Appl. Phys. Lett.*, 2009, **95**, 163108.
23. B. Zhao, G. Shao, B. Fan, W. Zhao and R. Zhang, *Phys. Chem. Chem. Phys.*, 2015, **17**, 2531-2539.
24. Z. Yang, Z. Li, L. Yu, Y. Yang and Z. Xu, *J. Mater. Chem. C*, 2014, **2**, 7583-7588.
25. C. Wang, X. Han, X. Zhang, S. Hu, T. Zhang, J. Wang, Y. Du, X. Wang and P. Xu, *J. Phys. Chem. C*, 2010, **114**, 14826-14830.